Cell Reports, Volume *37*

Supplemental information

Stabilized coronavirus spike stem elicits a broadly protective antibody

Ching-Lin Hsieh, Anne P. Werner, Sarah R. Leist, Laura J. Stevens, Ester Falconer, Jory A. Goldsmith, Chia-Wei Chou, Olubukola M. Abiona, Ande West, Kathryn Westendorf, Krithika Muthuraman, Ethan J. Fritch, Kenneth H. Dinnon III, Alexandra Schäfer, Mark R. Denison, James D. Chappell, Ralph S. Baric, Barney S. Graham, Kizzmekia S. Corbett, and Jason S. McLellan

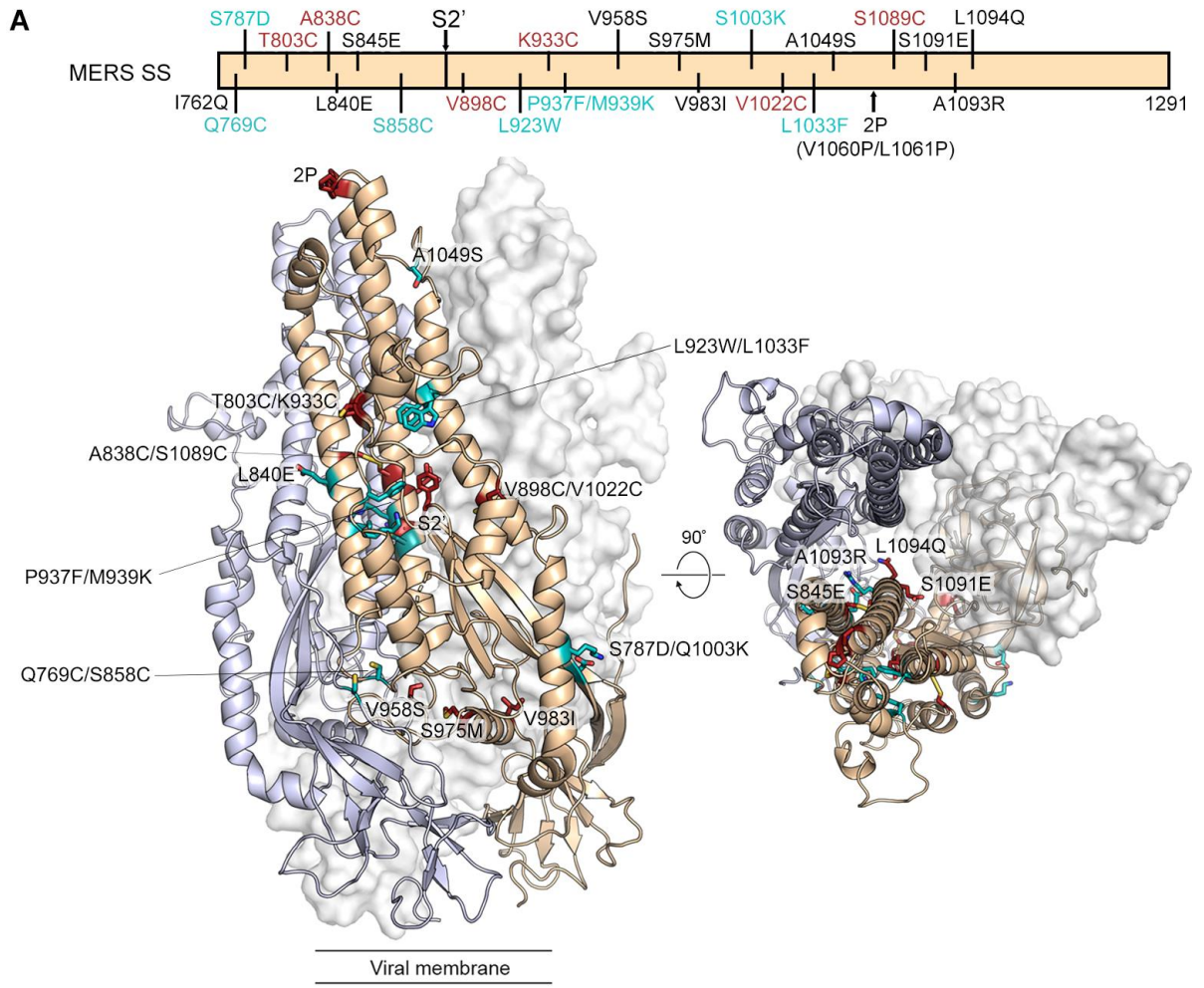
A
MERS SS
S787D
A838C
T803C
S845E
S2'
K933C
V958S
S975M
S1003K
A1049S
S1089C
S1091E
L1094Q
I762Q
Q769C
L840E
S858C
V898C
P937F/M939K
L923W
V983I
V1022C
L1033F
2P
(V1060P/L1061P)
A1093R
1291
2P
A1049S
L923W/L1033F
T803C/K933C
A838C/S1089C
L840E
V898C/V1022C
S2'
P937F/M939K
Q769C/S858C
S787D/Q1003K
V958S
S975M
V983I
90°
A1093R
L1094Q
S845E
S1091E
Viral membrane

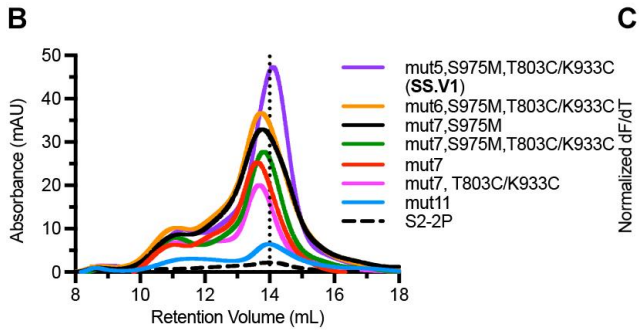
B
Absorbance (mAU)
Retention Volume (mL)
mut5,S975M,T803C/K933C (SS.V1)
mut6,S975M,T803C/K933C
mut7,S975M
mut7,S975M,T803C/K933C
mut7
mut7, T803C/K933C
mut11
S2-2P

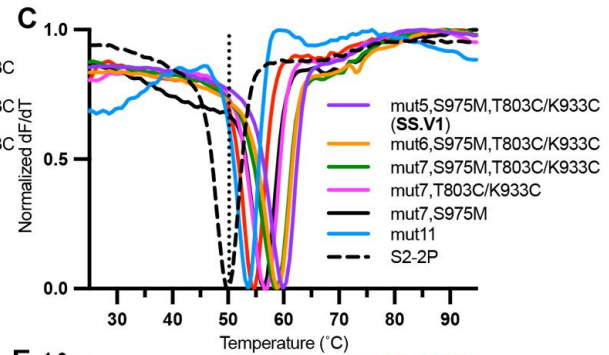
C
Normalized dF/dT
Temperature (°C)
mut5,S975M,T803C/K933C (SS.V1)
mut6,S975M,T803C/K933C
mut7,S975M,T803C/K933C
mut7,T803C/K933C
mut7,S975M
mut11
S2-2P

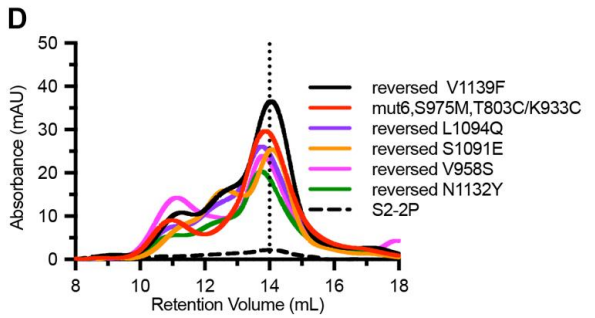
D
Absorbance (mAU)
Retention Volume (mL)
reversed V1139F
mut6,S975M,T803C/K933C
reversed L1094Q
reversed S1091E
reversed V958S
reversed N1132Y
S2-2P

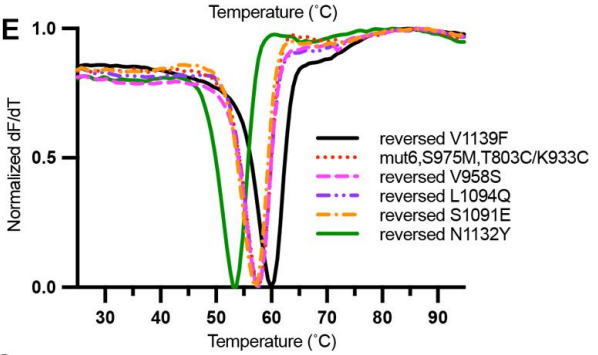
E
Normalized dF/dT
Temperature (°C)
reversed V1139F
mut6,S975M,T803C/K933C
reversed V958S
reversed L1094Q
reversed S1091E
reversed N1132Y

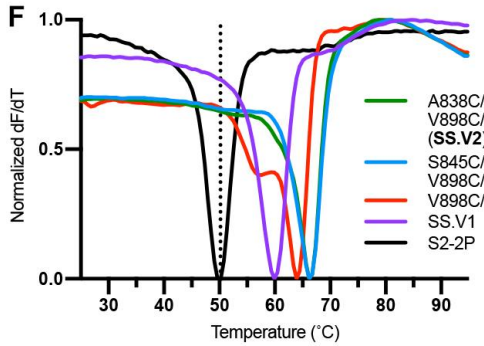
F
Normalized dF/dT
Temperature (°C)
A838C/S1089C, V898C/V1022C (SS.V2)
S845C/A1096C, V898C/V1022C
V898C/V1022C
SS.V1
S2-2P

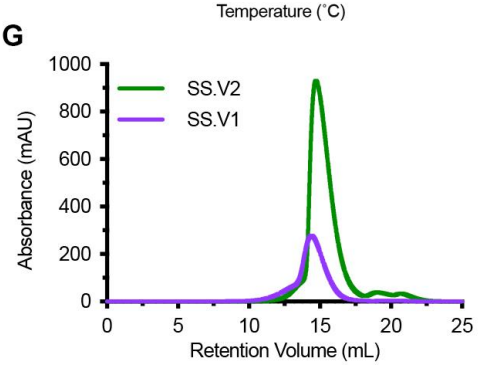
G
Absorbance (mAU)
Retention Volume (mL)
SS.V2
SS.V1

Figure S1. Designed substitutions for MERS-CoV stem stabilization, Related to Figure 1.
(A) Schematic of MERS-CoV stabilized stem primary structure, highlighted with beneficial single substitutions (top panel). Following the artificial signal peptide, the residue 762 in all our constructs is substituted with Gln to enhance cleavage efficiency of the signal peptidase. The trimerization motif (foldon) and affinity tags are fused to the carboxy terminus of the last residue 1291. The paired substitutions of the design are colored the same in red or cyan. S2′= S2′ protease cleavage site. Side and top view of the modeled MERS-CoV S structure (PDB ID: 5W9I) with S1 subunit omitted. To highlight the inter-protomer disulfide design, two protomers of the S2 subunits are shown as a ribbon diagram with the other one protomer shown in a transparent molecular surface (bottom panel). The substitutions in SS.V1 and SS.V2 are colored in red, and all other beneficial substitutions shown are colored in cyan.
(B,C) size-exclusion chromatography (SEC) and differential scanning fluorimetry (DSF) analysis for reversed and combinational-substitution S variants. Mut5, mut6 and mut7 have six, five and four residues of mut11 reversed to the wild-type, respectively. S975M and T803C/K933C are additional mutations combined with mut5, mut6 and mut7.
(D,E) SEC and DSF analysis for S variants. Each substitution in mut6,S975M,T803C/K933C backbone is respectively reversed to the wild-type residue.
(F) DSF analysis for combinatorial disulfide-substituted S variants, generated by adding additional one or two disulfide substitutions on MERS SS.V1 backbone.
In (B) and (D), a vertical dotted line indicates the peak retention volume for S2-2P. In (C) and (F), a vertical dotted line indicates the apparent melting temperature for S2-2P.
(G) SEC traces of MERS SS.V1 and MERS SS.V2 purified from a 1 L culture of FreeStyle 293F cells.

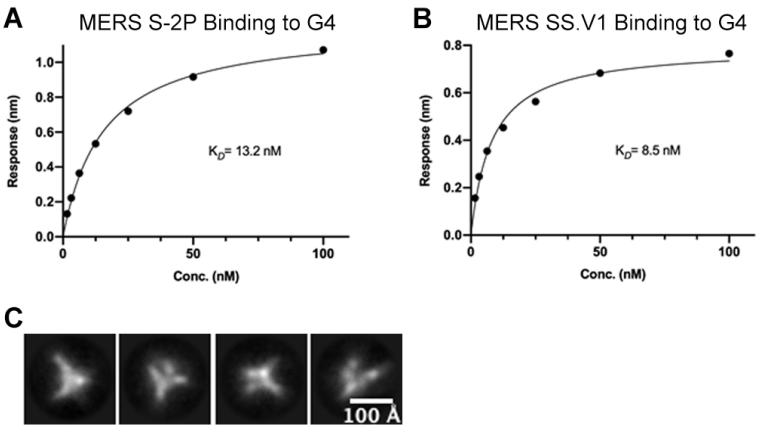

Figure S2. MERS S-2P and MERS SS.V1 exhibit nanomolar binding affinity to mAb G4, Related to Figure 1.

(A-B) Binding of (A) MERS-CoV S-2P or (B) MERS-CoV SS.V1 to mAb G4 assessed by biolayer interferometry (BLI). AHC sensor tips were used to capture mAb G4 and then dipped into a well containing MERS S-2P or MERS SS in BLI buffer. The end-point binding responses were plotted against concentrations of S, and the best fit by steady state analysis is shown as a nonlinear line.
(C) Representative 2D class averages of Fab G4 complexed with MERS SS.V1 by negative stain electron microscopy (nsEM).

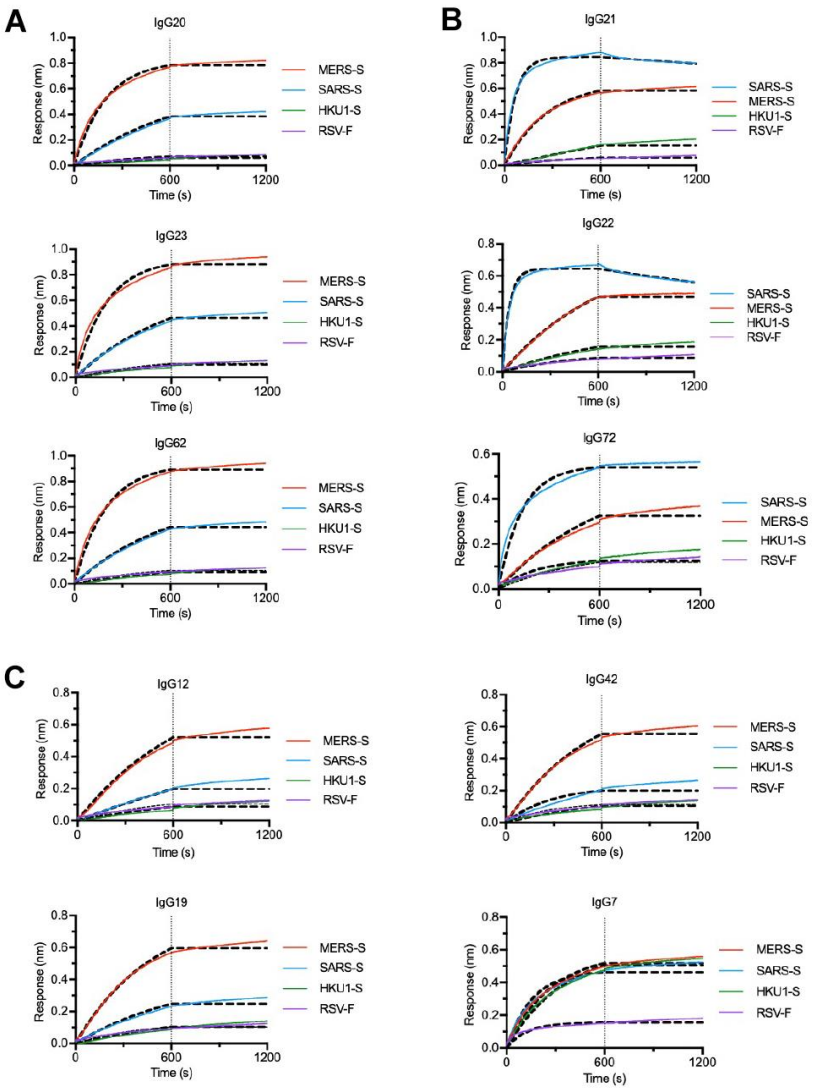

Figure S3. MERS SS.V1 elicited mAbs exhibit a spectrum of the binding specificities to betacoronavirus S proteins, Related to Figures 2 and 4.

(A-C) Binding of MERS SS.V1 elicited mAbs to MERS-CoV S, SARS-CoV S, HCoV-HKU1 S assessed by BLI. RSV-F containing a consensus trimerization motif (foldon) is also included as a negative control. Binding data are shown as red lines (MERS-S), blue lines (SARS-S), green lines (HKU1-S), purple lines (RSV-F), and the best fit to a 1:1 binding model is shown as dash lines. A vertical dotted line indicates the end of the binding event. The selected mAbs are grouped by their binding kinetics: (A) bi-specificity, faster on rates to MERS-S than SARS-S (B) bi-specificity, faster on rates to SARS-S than MERS-S (C) only binding to MERS-S or only binding to foldon.

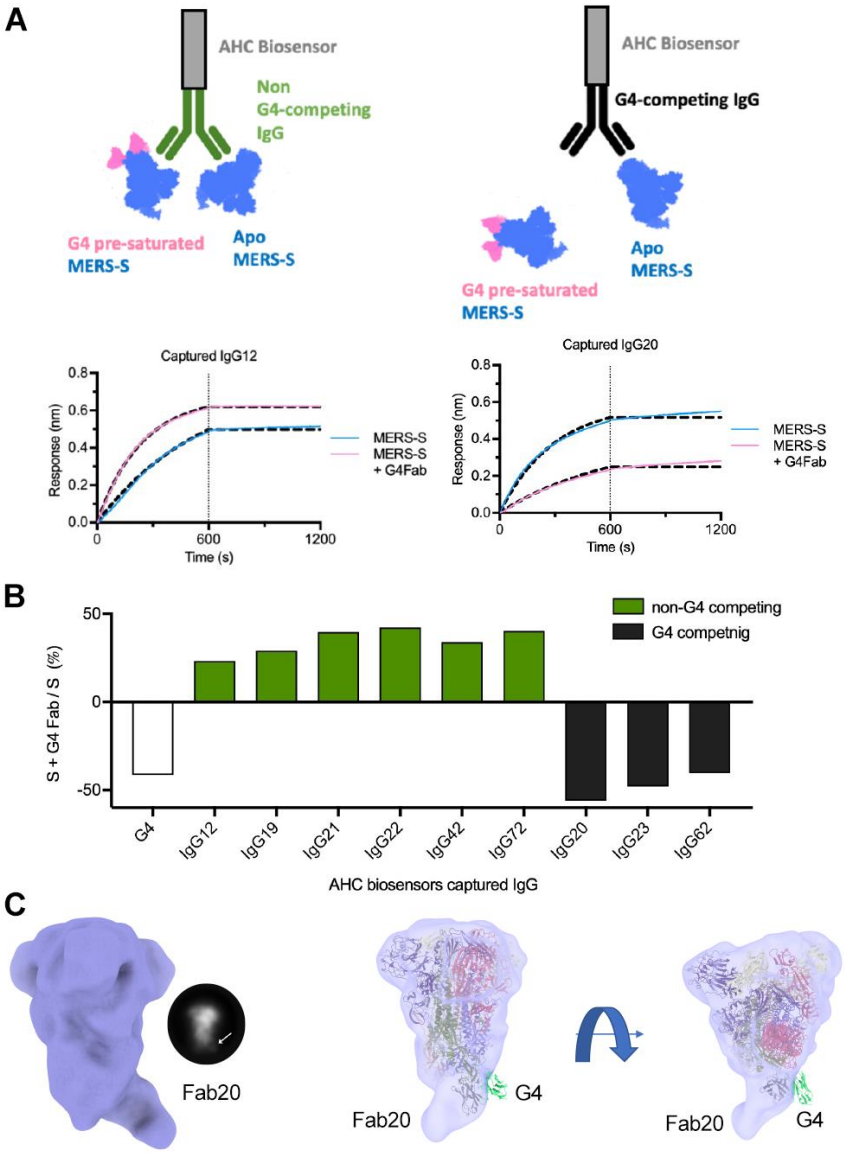

Figure S4. Two third of MERS SS.V1 elicited mAbs bind to the regions other than G4 binding loop, Related to Figures 2 and 4.

(A) Illustration of the scheme of experimental design for G4 competition assay by BLI. AHC biosensors were used to capture selected mAb and then dipped into G4 Fab pre-saturated MERS-S or apo MERS-S. Binding data are shown as pink lines (G4 Fab pre-saturated MERS-S) and blue lines (apo MERS-S) and the best fit to a 1:1 binding model is shown as dash lines. A vertical dotted line indicates the end of the binding event when the responses are used for end-point binding analysis.

(B) End-point binding responses of mAbs to G4 Fab pre-saturated MERS-S versus MERS-S are calculated and shown as percentage. mAb G4 is also included as a control (white bar). Non-G4 competing mAbs having higher responses to G4 Fab pre-saturated MERS-S than MERS-S are depicted as green bars. G4 competing mAbs having higher responses to MERS-S than G4 Fab pre-saturated MERS-S are depicted as black bars.

(C) A representative 2D class average and reconstructed 3D volume of a non-G4-competing antibody, Fab20, complexed with MERS-S. The G4 (green) bound MERS-S model (PDB: 5W9J) is docked into the EM map of the Fab20–MERS-S complex.

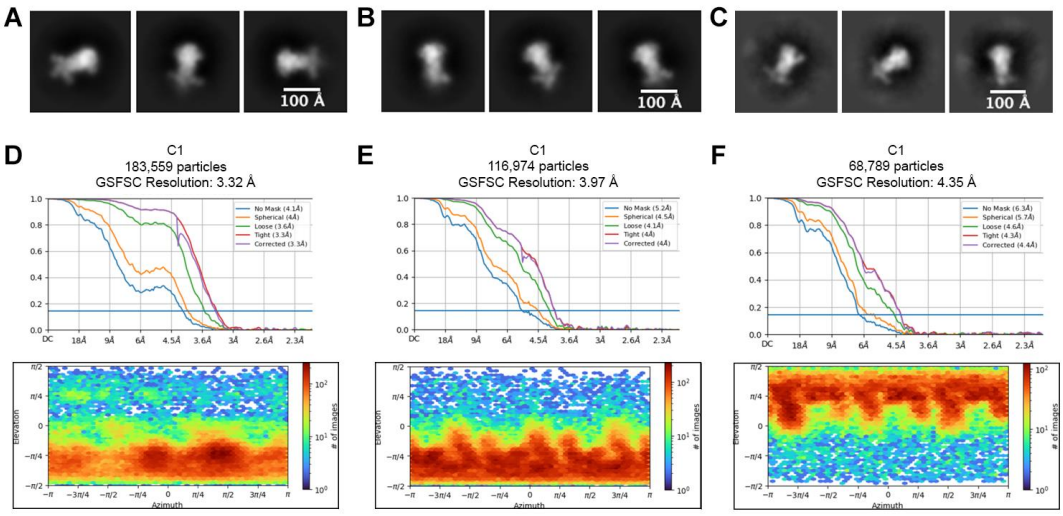

Figure S5. EM analysis of stem-targeted antibodies and cryo-EM structure validation. Related to Figures 4 and 5.

(A) Representative 2D class averages of Fab22 complexed with MERS-CoV S by negative stain electron microscopy (nsEM).

(B) Representative 2D class averages of Fab72 complexed with MERS-CoV S by nsEM.

(C) Representative 2D class averages of Fab22 complexed with HexaPro, a prefusion stabilized SARS-CoV-2 S, by nsEM.

(D-E) FSC curves and viewing distribution plots for (D) MERS-CoV S-Fab 22 structure, (E-F) SARS-CoV-2 S-Fab 22 structures with (E) 1-RBD up and (F) 3-RBD down generated in cryoSPARC v2.15.

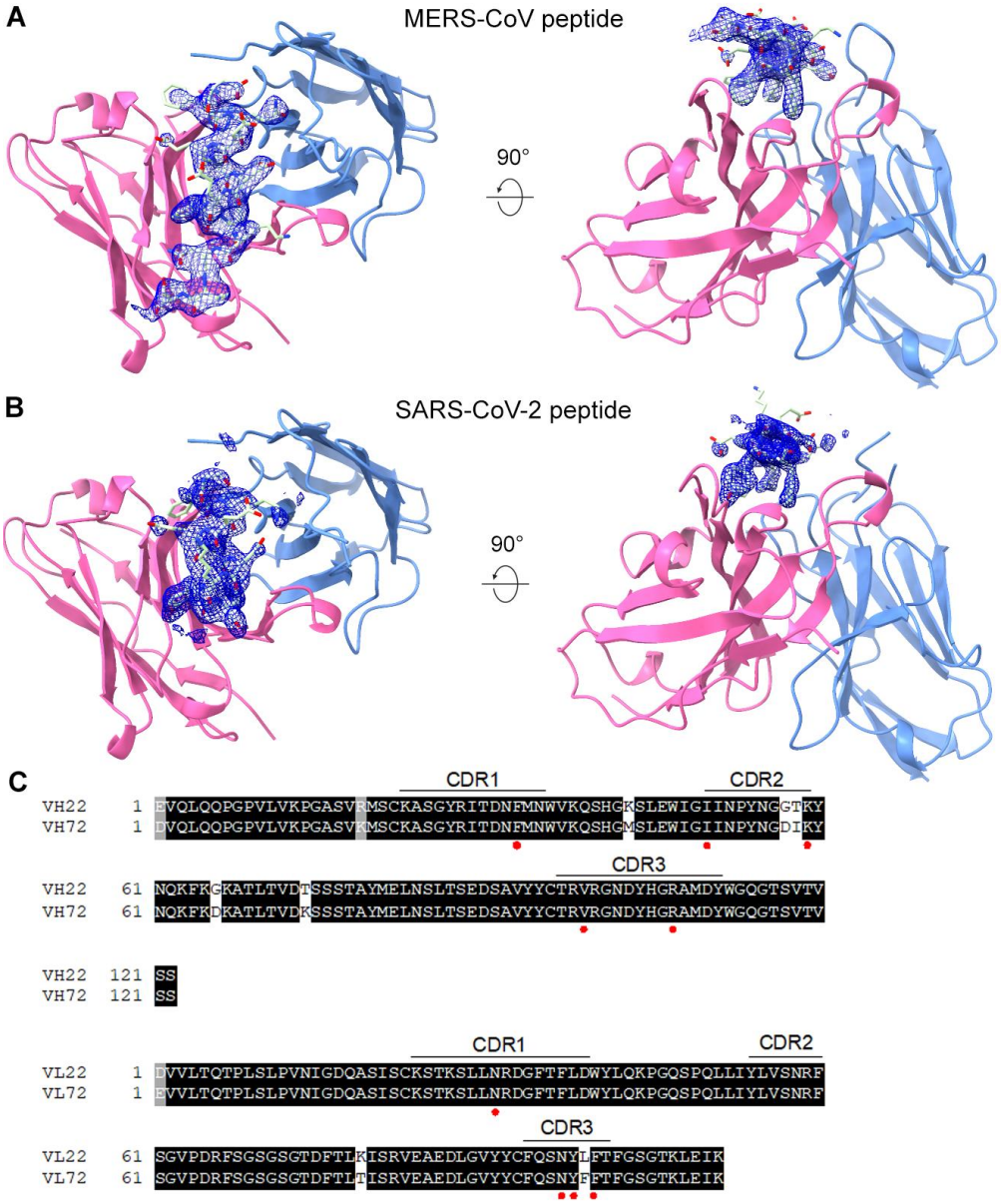

Figure S6. Electron density for stem helix peptides and sequence alignments of stem-targeted antibodies, Related to Figure 6.

(A,B) Fab22 from the complex with MERS-CoV (A) and SARS-CoV-2 (B) stem helix peptides is shown as cartoon representation and the same color scheme as Figure 7. Stem helix peptides are shown as light green sticks, with oxygens colored red and nitrogens colored blue. The isolated electron density for each peptide (2Fo-Fc) is shown as a dark blue mesh.

(C) Sequence alignments of variable domains of IgG22 and IgG72. The key residues involved in the binding interfaces of Fab22 and the S2 stalk peptides are denoted in red circles.

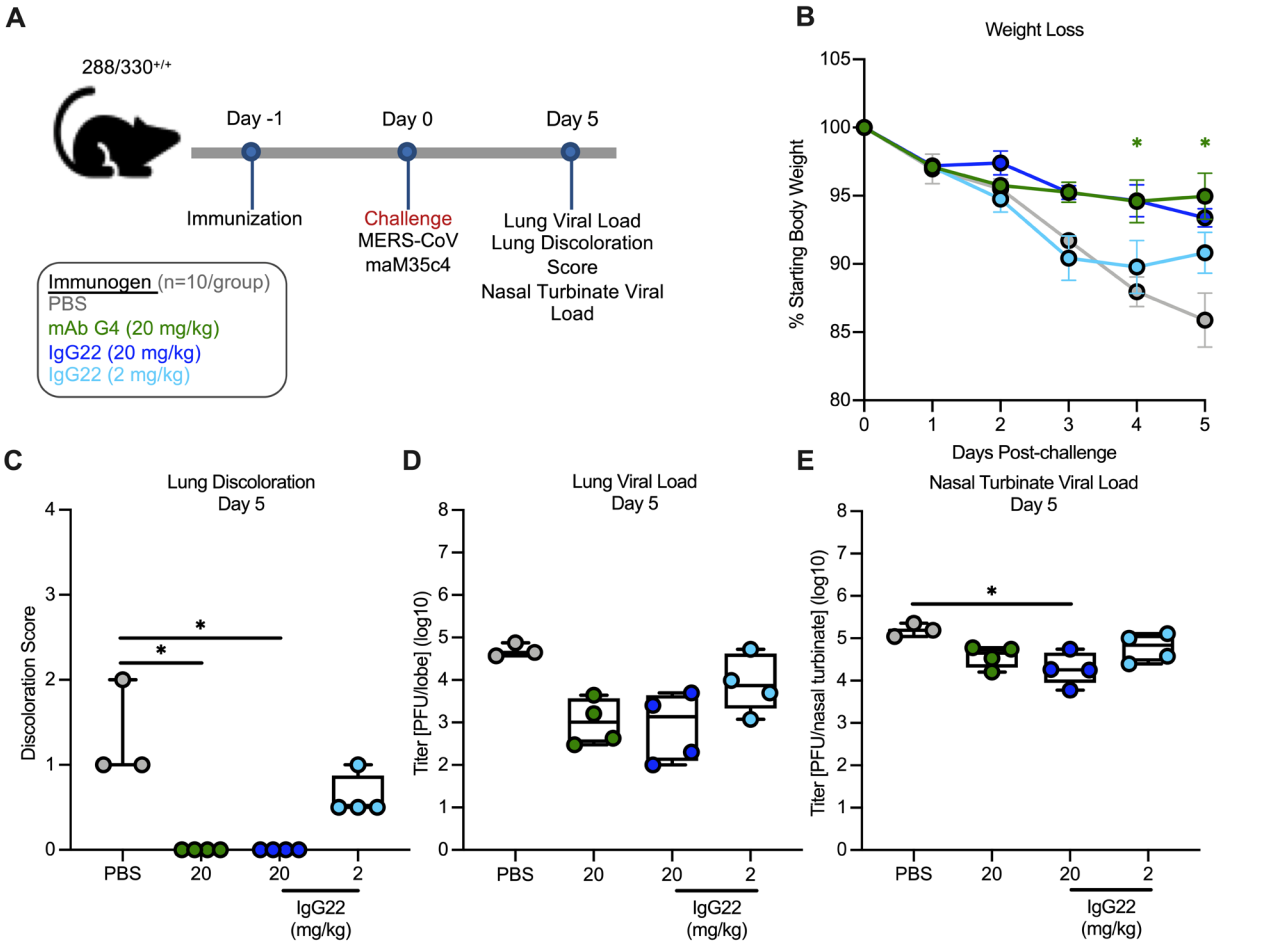

Figure S7. Passive transfer of IgG22 protects mice from lethal MERS-CoV challenge, Related to Figure 7.
(A) 288/330+/+ mice were treated with 20 mg/kg of mAb G4 (green), 20 mg/kg of IgG22 (blue), or 2 mg/kg (light blue) intraperitoneally on the day before challenge.
(B) Following challenge, mice were monitored for weight loss out to 5 days post-challenge. Each symbol represents the mean, and error bars represent the SEM of each group per day. Groups were compared to the PBS control via One-Way ANOVA with Kruskal-Wallis post-test.
(C-E) On day 5 post-challenge, mice were sacrificed and assessed for (C) lung discoloration (0 = no discoloration, 4 = severe discoloration in all lobes), and for both (D) lung and (E) nasal turbinate viral load. Circles indicate individual animals and black lines indicate the median Groups were compared to each other via One-Way ANOVA with multiple comparisons (C-H). * = $p < 0.05$, ** = $p < 0.01$.

Table S1. Cryo-EM data collection and processing statistics, Related to Figures 4 and 5.

EM data collection		
Microscope	FEI Titan Krios	FEI Titan Krios
Voltage (kV)	300	300
Detector	Gatan K3	Gatan K3
Magnification (nominal)	22500	22500
Pixel size (Å/pix)	1.1	1.1
Flux (e^-/pix/sec)	8.0	9.1
Frames per exposure	80	30
Exposure (e^-/Å^2)	80	37.2
Defocus range (mm)	1.0-2.5	1.0-2.5
Micrographs collected	2,383	2,013
Sample	MERS-CoV S + Fab 22	SARS-CoV-2 S + Fab 22

3D reconstruction statistics			
	3-RBD down	1-RBD up	3-RBD down
Particles	89,372	119,974	68,789
Symmetry	C1	C1	C1
Map sharpening B-factor	-78.4	-135.8	-159.1
Unmasked resolution at 0.143 FSC (Å)	4.10	5.20	6.30
Masked resolution at 0.143 FSC (Å)	3.29	3.97	4.35

Table S2. Crystallographic data collection and refinement statistics, Related to Figure 6.

	Fab22+MERS-CoV peptide	Fab22+SARS-CoV-2 peptide
PDB ID	7S3M	7S3N
Data collection		
Space group	$P3_121$	$C2$
Wavelength (Å)	0.979	0.979
Cell dimensions		
a, b, c (Å)	123.2, 123.2, 97.2	80.66, 72.89, 89.06
α, β, γ (°)	90, 90, 120	90, 100.4, 90
Resolution (Å)	71.84-2.40 (2.49-2.40)	87.55-1.90 (1.94-1.90)
R_{merge}	0.114 (1.384)	0.136 (0.325)
$I / \sigma I$	9.8 (1.8)	5.1 (2.0)
$CC_{1/2}$	0.988 (0.927)	0.987 (0.878)
Completeness (%)	100 (100)	97.3 (90.1)
Redundancy	8.8 (8.7)	3.6 (2.9)
Total reflections	297,776 (30,584)	139,727 (6,710)
Unique reflections	33,665 (3,507)	38,944 (2,343)
Refinement		
Resolution (Å)	53.33-2.40 (2.48-2.40)	43.78-1.90 (1.95-1.90)
Unique reflections	33,329 (2,983)	38,919 (2,682)
R_{work} / R_{free} (%)	21.7/25.7	18.2/22.1
No. atoms	3,507	3,739
Protein	3,587	3,420
Water	20	319
B-factors (Å^2)		
Protein	75.4	39.7
Water	62.1	41.5
R.m.s. deviations		
Bond lengths (Å)	0.006	0.015
Bond angles (°)	0.93	1.50
Ramachandran (%)		
Favored	96.1	96.7
Allowed	3.9	3.3
Outliers	0.0	0.0

Each dataset was collected from one crystal.
*Values in parentheses are for highest-resolution shell.